Current Research (2026) Newfoundland and Labrador Department of Energy and Mines Geological Survey, Report 26-1, pages 235-253

PRELIMINARY INVESTIGATIONS OF THE NORTH RED WINE PLUTON, LABRADOR

Z. Magyarosi and A. Hosson[1]
Mineral Deposits Section
[1]Department of Earth Sciences, Memorial University of Newfoundland, St. John's, NL

ABSTRACT

Labrador hosts several ~1.3-Ga rare-earth-element (REE)-mineralized, alkaline-silicate igneous systems, including the Strange Lake and Flower River complexes, the Red Wine Intrusive Suite (RWIS) and the Fox Harbour Belt and associated rocks. Among these systems, RWIS is the most evolved as indicated by the presence of agpaitic units. Previous studies on the RWIS provided valuable data but also revealed significant uncertainties due to the uncommon characteristics of these rocks and later deformation and metamorphism. This report presents field relationships and geochemical analysis of 76 samples from the silica-undersaturated units of the North Red Wine pluton, as well as detailed petrography, SEM analysis, X-ray maps and modal mineralogy of five representative samples.

The identified rock types include nepheline-bearing pulaskite, nepheline-bearing malignite, lujavrite and malignite. The main minerals are albite, K-feldspar, nepheline, eudialyte, pyroxene, amphibole, aenigmatite, pectolite, britholite and an unidentified Ca–K–Zr–Si phase. Rare-earth elements are hosted in eudialyte, occurring as a primary magmatic phase, and britholite, which formed later through magmatic or hydrothermal processes.

The RWIS was metamorphosed and deformed during the Grenville orogeny. The rocks are folded, foliated and locally lineated. However, some of these fabrics are most likely primarily magmatic as suggested by their occurrence in undeformed agpaitic intrusions. Previous studies have estimated the metamorphic grade to be amphibolite facies, but this study suggests that there are several inconsistencies with this estimation, and therefore, the grade of metamorphism remains indeterminate.

Whole-rock geochemistry indicates that most of the samples are nepheline syenite. They are A-type, ferroan and peralkaline (AI≤2.9). On chondrite-normalized plots, the REE display moderate to weak inclined negative slopes from La to Lu. REE concentrations correlate positively with Zr, As, Mn, Pb and Zn.

INTRODUCTION

The Red Wine Intrusive Suite (RWIS) is one of a number of alkaline-silicate systems in Labrador that also include the Strange Lake and Flower River complexes, and the Fox Harbour Belt and associated rocks. These systems are *ca.* 1.3 Ga old and are commonly associated with significant rare-earth element (REE) and high-field-strength element (HFSE) mineralization (Miller *et al.*, 1997; Crocker, 2014; Ducharme *et al.*, 2021; Magyarosi and Rayner, 2025). This study is part of a multi-year project focusing on REE mineralization in alkaline-silicate systems in Labrador. The goal is to advance our understanding of the genesis of REE mineralization in these rocks and support exploration efforts for this deposit type.

Alkaline-silicate systems are characterized by the presence of alkaline or peralkaline rocks, even if they are dominated by metaluminous rocks (Beard *et al.*, 2022). They represent major sources of REE and HFSE, most of which are considered critical. Enrichment in REE, HFSE and other incompatible elements, including volatiles, results from low-degree melting of a metasomatized mantle, followed by extensive fractional crystallization and late magmatic processes. Peralkaline rocks are characterized by an agpaitic index (AI = molar (Na+K)/Al) greater than 1 and the presence of Na-rich amphiboles and/or pyroxenes. They are subdivided into miaskitic and agpaitic based on their HFSE mineralogy (Marks and Markl, 2017). Miaskitic rocks (AI≥1) contain zircon and titanite as the main HFSE minerals, whereas agpaitic rocks (AI>1.2) host HFSE in halogen-bearing complex Na–Ca minerals such as eudialyte-group minerals. Agpaitic rocks are considerably rarer than miaskitic rocks; within an alkaline magmatic province only a few localities evolve to agpaitic compositions, and they are generally less understood.

In Labrador, the RWIS is the most evolved alkaline-silicate system indicated by its agpaitic character. Although agpaitic assemblages occur in the Strange Lake complex, they are restricted to pegmatites indicating formation in late magmatic stage (Marks and Markl, 2017; Vasyukova and Williams-Jones, 2018). In contrast, agpaitic assemblages in the RWIS formed during the early magmatic stage, as indicated by the primary magmatic occurrence of typical agpaitic minerals such as eudialyte. In addition to the rare and unusual nature of the rocks, the geology of the RWIS is further complicated by metamorphism and deformation during Grenville orogeny *ca.* 1.0 Ga.

The RWIS has been the subject of several major studies (*see* Singh, 1972; Curtis and Currie, 1981; Crocker, 2014), following its discovery in the 1950s (Singh, 1972). While these investigations provided valuable data, they also highlighted significant uncertainties due to the unusual nature of these rocks and even basic rock identification and nomenclature have proven challenging. Historically, point counting was used for modal mineralogy, but this approach often led to errors because of the difficulty in distinguishing some of the uncommon minerals. In some cases, authors applied metamorphic terminology to magmatic rocks of the RWIS (*e.g.*, "leucocratic gneiss"; Curtis and Currie, 1981). In addition, the nomenclature of the silica-undersaturated rocks is not consistent, commonly named after a locality with no well-established modal mineralogy or whole-rock geochemistry data (Le Maitre *et al.*, 2002; Mikhailova *et al.*, 2020; Lustrino and Bonin, 2024).

This report summarizes the first year of work on the RWIS and includes field relationships and geochemical analysis of 76 samples from the North Red Wine pluton (NRW), as well as detailed petrography, SEM analysis, X-ray maps and modal mineralogy of five representative samples. This study aims to fill gaps of knowledge in the geology of the RWIS and compare it to other alkaline-silicate systems in Labrador and agpaitic rocks worldwide. Ongoing work includes Nd–Sm isotopic analysis, mineral and whole-rock chemistry to determine the relative timing of units and processes (*e.g.*, magmatic, hydrothermal, metamorphic), reassessment of metamorphic grade, alteration, and additional geochronology.

GEOLOGICAL SETTING

REGIONAL GEOLOGY

The RWIS is located in the Grenville Province, within the Grenville Front Zone, south of the boundary with the Churchill Province (Figure 1; Gower *et al.*, 1980). The oldest units in the Red Wine area include the Paleoproterozoic Disappointment Lake Gneiss, consisting of quartzo-feldspathic gneisses, intruded by the Trans-Labrador batholith, consisting of foliated granite to quartz monzonite. The Trans-Labrador batholith was dated at 1655 ± 11 and 1658 ± 13 Ma using Rb/Sr in whole rock (Fryer, 1983).

Mesoproterozoic units include the Letitia Lake Group (LLG), the RWIS and the Seal Lake Group (Figure 1). The LLG has been subdivided into a lower unit consisting of quartz–feldspar and feldspar porphyritic rocks, a middle unit consisting of peralkaline rhyolite (porphyritic, banded and tuffaceous) and an upper unit consisting of phyllite and greywacke (Thomas, 1981). It has been dated at 1327 +4/-2 Ma with U/Pb in zircon (Fryer, 1983) and is closely related to the RWIS based on mineralogy, geochemistry, and spatial and temporal association (Hill and Thomas, 1983; Hill and Miller, 1990). The LLG hosts the Two Tom Lake, Green Arrow, Mann #1 and Mann #2 occurrences (Figure 1, Table 1). Miller (1987) interpreted the mineralization to be related to intrusions of the RWIS within the LLG and described five types of mineralization based on prevalent mineralogy. An NI 43-101-compliant inferred mineral resource for Two Tom Lake indicates 41 Mt at 1.18% total REE oxides (TREO), 0.26% Nb_2O_5, 0.18% BeO and 0.06 ThO_2% with 5% of the TREO being made up of heavy-rare-earth-element oxides (HREO) (Daigle, 2012).

The Mesoproterozoic Seal Lake Group comprises arenaceous and argillaceous sedimentary rocks and amygdaloidal and massive basalt flows intruded by gabbro sills (Figure 1; van Nostrand and Corcoran, 2013). The age of the Seal Lake Group ranges between *ca.* 1270 and 1225 Ma (Cadman *et al.*, 1993; Romer *et al.*, 1995).

The Red Wine area was affected by metamorphism and deformation during the Grenville orogeny (Thomas, 1981). The Disappointment Lake Gneiss records three deformational events, whereas the Trans-Labrador batholith preserves evidence of only one. The RWIS was affected by at least two deformational events, although locally undeformed zones were noted. The Seal Lake Group underwent three deformational events, while the LLG shows evidence for only two.

The metamorphic grade in the region increases from north to south (Thomas, 1981; van Nostrand and Corcoran, 2013). In the Seal Lake Group, it ranges from unmetamorphosed in the north to greenschist facies in the south (van Nostrand and Corcoran, 2013). The grade of metamorphism in the LLG ranges from lower greenschist to upper greenschist facies from north to south (Thomas, 1981). The grade of metamorphism in the older Paleoproterozoic rocks ranges from middle greenschist to upper greenschist in the Trans-Labrador batholith and upper amphibolite in the Disappointment Lake Gneiss (Thomas, 1981).

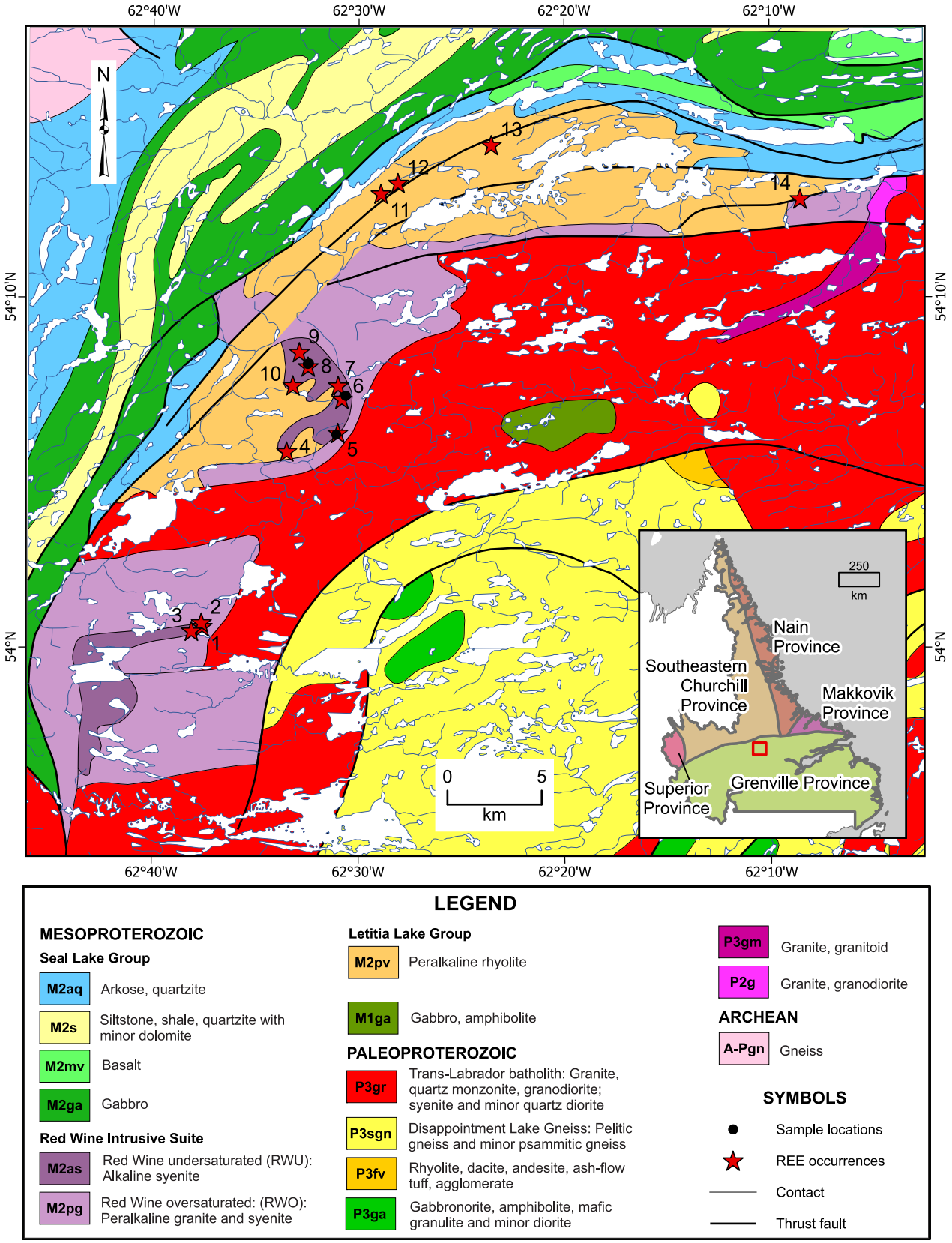

Figure 1. *Geology of the Red Wine area, central Labrador (after Wardle* et al.*, 1997).* See *Table 1 for the list of REE and HFSE occurrences in the RWIS.*

Table 1. REE and HFSE occurrences in the RWIS shown in Figure 1

Number	Occurrence name	Commodities
1	Playfair South #1	REE, Zr
2	Playfair South #2	REE, Zr
3	Playfair South #3	REE, Zr
4	Zinfandel	REE, Nb, Y, Zr
5	Pinot Rose	REE, Nb, Y, Zr
6	Cabernet	REE, Nb, Y, Zr
7	Malbec	REE, Nb, Y, Zr
8	Merlot	REE, Nb, Y, Zr
9	North Red Wine	REE, Zr, Be
10	Shiraz	REE, Nb, Y, Zr
11	Green Arrow	REE
12	Mann #2	Nb, Th, Be, Zn, REE
13	Mann #1	Be, Nb, U, Zn
14	Two Tom Lake	REE

RED WINE INTRUSIVE SUITE

The RWIS consists of the North Red Wine (NRW) and South Red Wine (SRW) plutons as well as several smaller bodies that host several REE occurrences (Table 1). It is composed of both silica-oversaturated units (Red Wine Oversaturated – RWO), formerly known as "Arc Lake gneisses" (Curtis and Currie, 1981), and silica-undersaturated units (Red Wine Undersaturated – RWU). The RWU intrude and are surrounded by the RWO, the Letitia Lake Group (LLG), and the Disappointment Lake Gneiss. Rock types in the RWO include peralkaline granites (Curtis and Currie, 1981).

The RWU is variable in composition, and previous authors have subdivided it into various rock types based mainly on their mineralogy (Singh, 1972; Curtis and Currie, 1981). Singh (1972) subdivided the RWU into ijolite–urtite, lujavrite, nepheline syenite and "eudialytite", a rock composed of 60 to 80% eudialyte, the latter one occurring as veins and patches in nepheline syenite. Curtis and Currie (1981) divided them into green melanocratic gneiss (lujavrite), blue-black melanocratic gneiss, leucocratic gneiss, arfvedsonite melteigite, nepheline syenite and malignite and hybrid syenites, whereas Crocker (2014) simply subdivided rocks of the RWU into leucocratic and melanocratic syenites.

The RWU consist of varying proportions of feldspars, nepheline, pyroxene, amphibole, aenigmatite and eudialyte as the essential minerals (Singh, 1972; Curtis and Currie, 1981; Crocker, 2014). In the RWU, five types of pyroxenes have been identified; aegirine, calcic aegirine, titanian aegirine, aegirine–jadeite and titaniferous ferro-omphacite (Curtis and Gittins, 1979). The amphiboles are arfvedsonite in the RWU, in contrast to riebeckite in the RWO. In addition to the major rock-forming phases, numerous other minerals, several of which are very rare, have been described (Singh, 1972; Curtis and Currie, 1981). The main REE minerals are eudialyte, occurring as a primary magmatic phase, and britholite, described as a secondary phase (Crocker, 2014).

Dating of the RWO using Rb/Sr in whole rocks returned 1265 ± 75 Ma (Curtis and Currie, 1981) and with U/Pb in zircon and titanite 1337 +10/-8 Ma (Gandhi *et al.*, 1988). Dating the silica-undersaturated rocks has been difficult due to lack of suitable minerals. Rb/Sr in whole rocks returned 1345 ± 75 Ma (Blaxland and Curtis, 1977), which was later recalculated to 1317 ± 75 Ma (Thomas, 1993). K/Ar in various minerals returned ages ranging from 1417 ± 102 to 1207 ± 75 Ma (Singh, 1972). In addition, all studies returned metamorphic ages around 1.0 Ga including the most recent attempts by Crocker (2014) using U/Pb in eudialyte and britholite.

The RWIS occurs as folded and deformed masses within the country rocks and show evidence of repeated deformation (Curtis and Currie, 1981). The direction of the foliation within the RWIS is very variable in orientation, but is generally consistent with the foliation of the country rocks. The RWIS have been subjected to more ductile rather than brittle deformation relative to the country rocks, which may have been due to its original high volatile content promoting recrystallization (Curtis and Currie, 1981).

The grade of metamorphism in the RWIS was estimated to be amphibolite facies based on the presence of Al-rich pyroxene (jadeite-rich) rims and the coexistence of jadeite with nepheline and albite (Curtis and Currie, 1981). However, changes in the grade of metamorphism are very sharp and occur in less than a few centimetres, concluding mechanical deformation to juxtapose them (Curtis and Currie, 1981). The stability of pyroxene rather than amphibole at amphibolite facies is explained by the dry and silica-poor nature of the rocks, and the lack of water during subsequent metamorphism.

ANALYTICAL METHODS

A total of 76 samples were collected from the NRW. Whole-rock geochemical analyses were completed at the geochemical laboratory of the Geological Survey of Newfoundland and Labrador (GSNL). Samples were cleaned, crushed, pulverized and analyzed (*see* Finch *et al.*, 2018). Polished thin sections of representative samples were examined using a petrographic microscope.

Five samples, representing the various rock types in the NRW, were selected for analysis using a FEI MLA 650FEG SEM at Memorial University of Newfoundland (MUN) Micro Analysis Facility (MUN MAFIIC). Qualitative analyses were completed using high throughput Energy-dispersive X-ray Spectroscopy (EDX) detectors from Bruker (https://www.mun.ca/creait/). SEM-MLA analysis was performed to produce false-colour X-ray maps of the samples and determine the abundances of minerals in the samples. The SEM-MLA uses backscattered electron imaging (BEI) to measure the average atomic number of the minerals to establish grain boundaries, then classifies the grains as minerals using a mineral reference list and allows quantitative evaluation of the abundances of minerals, among other characteristics.

RESULTS

FIELD RELATIONSHIPS

Both in composition and grain size, the rocks from NRW vary significantly at the outcrop scale (Plate 1A–D). Rock types are intricately intermixed, and transitions between units are commonly gradual, occurring over scales ranging from a few centimetres (Plate 1B) to several metres. Compositions range from melasyenite to leucosyenite occurring as layers or lenses, although mafic and intermediate rocks predominate. The principal ferromagnesian minerals are amphibole (black) and pyroxene (green), and the intermediate and mafic rocks typically alternate between amphibole-rich and pyroxene-rich layers on a centimetre- to metre-scale (Plate 1C).

Grain size is generally medium to coarse, varying between layers (Plate 1D) or changing irregularly in patches (Plate 1E). Pegmatites occur as layers, lenses or pockets (Plate 1A, F) and consist mainly of amphibole and feldspar (Crocker, 2014), with less common eudialyte and pyroxene; the latter is typically finer grained than amphibole. Most rocks are foliated, folded, and commonly display kink bands (Plate 1C); some are lineated, defined by amphibole (Plate 1G). Eudialyte is concentrated in layers in syenites (Plate 1H) but may also occur disseminated or within pegmatites.

PETROGRAPHY AND SEM ANALYSIS

The rock types selected for detailed petrographic, and SEM-MLA analyses include nepheline-bearing pulaskite, nepheline-bearing malignite and lujavrite with variable amounts of amphibole and pyroxene (Figure 2, Table 2). Malignite was not among the samples analyzed with SEM-MLA, but it was petrographically identified based on the increased amount of amphibole and/or pyroxene compared to lujavrite. The rock names are based on a preliminary report for classification and nomenclature of igneous rocks by Lustrino and Bonin (2024). The main minerals include albite, K-feldspar, nepheline, eudialyte, pyroxene, amphibole, aenigmatite, pectolite, britholite and an unidentified Ca–K–Zr–Si phase (Tables 2 and 3). Minerals present in trace amounts include sodalite, biotite, apatite, calcite, fluorite, galena, pyrite, sphalerite, synchysite and numerous unidentified phases (Table 2).

The amphibole and pyroxene contents vary gradually, and both minerals commonly coexist. In most of the samples, amphibole crystallized before pyroxene. Amphibole is K-bearing arfvedsonite (Curtis and Currie, 1981) and no changes in composition were detected by SEM. Pyroxene is typically zoned showing an increase in Al and decrease in Fe from core to rim. Curtis and Currie (1981) indicate that the composition of the pyroxenes ranges from aegirine and aegirine–jadeite to titanian ferro-omphacite with the more Al-rich compositions occurring towards the rim.

The main REE minerals are britholite and eudialyte (Tables 2 and 3). Eudialyte appears as a primary, early crystallizing phase, whereas britholite and other REE minerals occur as late phases, either magmatic or late-magmatic hydrothermal. The composition of britholite is highly variable, ranging from Ce-rich to Y-rich and from silicate to phosphate with some grains also containing Th (for more detail *see* Crocker, 2014).

Sample 24RW0006A01 is a coarse-grained, nepheline-bearing pulaskite consisting of mainly albite, K-feldspar, nepheline, amphibole, pyroxene, aenigmatite and pectolite (Plate 2A–C; Table 2). The main REE-bearing minerals include eudialyte and britholite and possibly apatite, all occurring in trace amounts. The order of crystallization is feldspar, aenigmatite, pectolite, amphibole, pyroxene and nepheline. Aenigmatite is dark red and is surrounded by pectolite, then amphibole, which is surrounded by pyroxene. The amphibole is green to brown. Pyroxene is an unusual bright blue (Plate 2C, D), which has been identified as Ti-rich omphacite (Curtis and Currie, 1981). Eudialyte forms subhedral crystals indicating that it crystallized early, possibly after aenigmatite and before amphibole. Feldspar occurs as euhedral to subhedral crystals up to 20 mm in length and consists of strongly albitized K-feldspar (Plate 2A, E). Nepheline contains inclusions of amphibole and less common pyroxene. Trace amount of sodalite and apatite also occur with nepheline.

Sample 24RW0006A03 is a pyroxene-rich nepheline-bearing malignite composed of eudialyte, K-feldspar, pyroxene, albite and amphibole as the main minerals (Plate 3A, Table 2). The sample contains an eudialyte-rich layer occur-

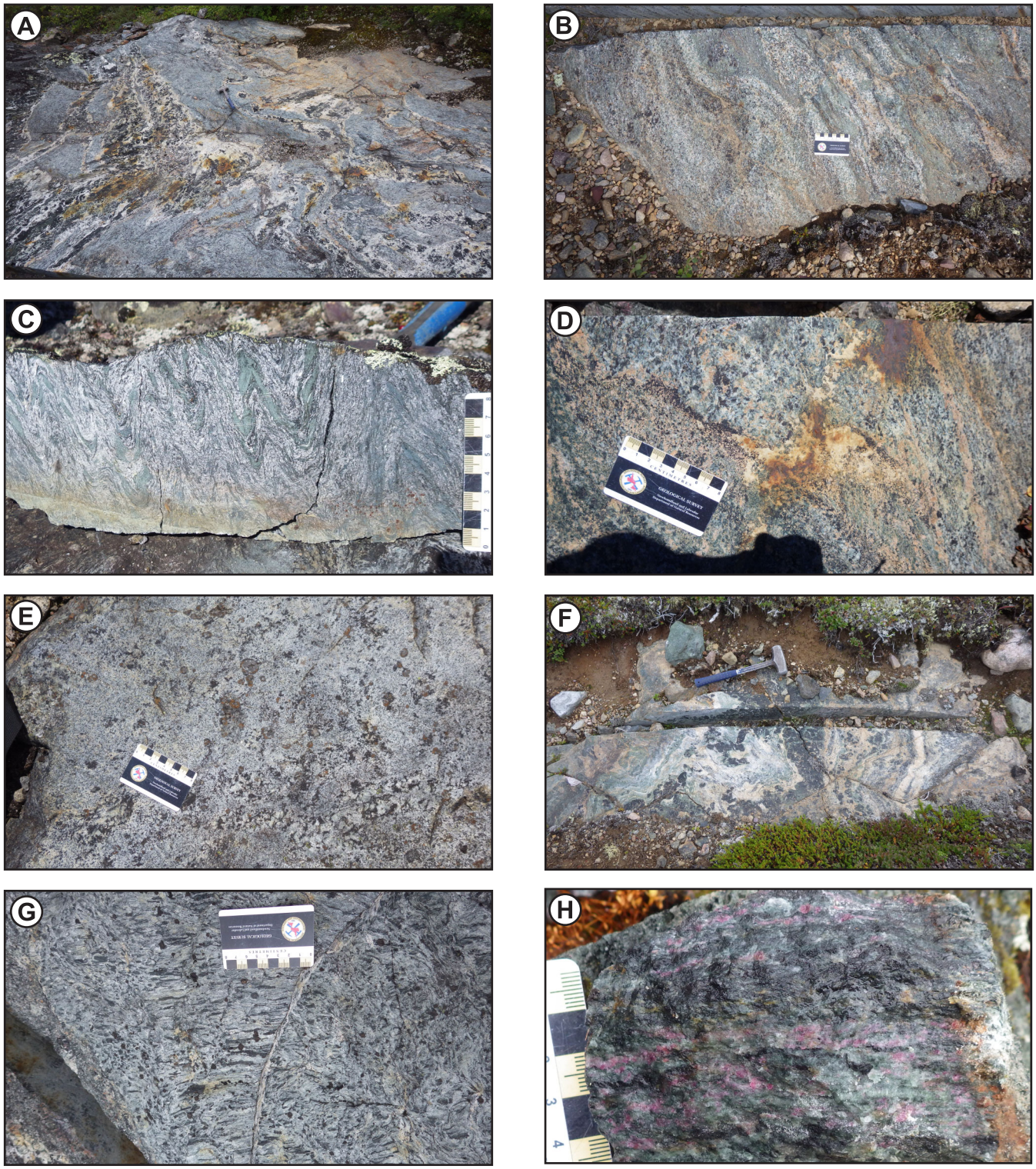

Plate 1. *Field photos from the NRW pluton of the RWIS. A) Pegmatite layers in melasyenites; B) Compositional layering; C) Kink folding in mixed amphibole (black) and pyroxene (green) lujavrite; D) Syenites having varying composition and grain size; E) Variation in grain size in leucosyenites; F) Pegmatite pocket composed of amphibole (black), pyroxene (green) and albite; G) Lineation defined by amphibole; H) Eudialyte (pink)-rich layers in melasyenites.*

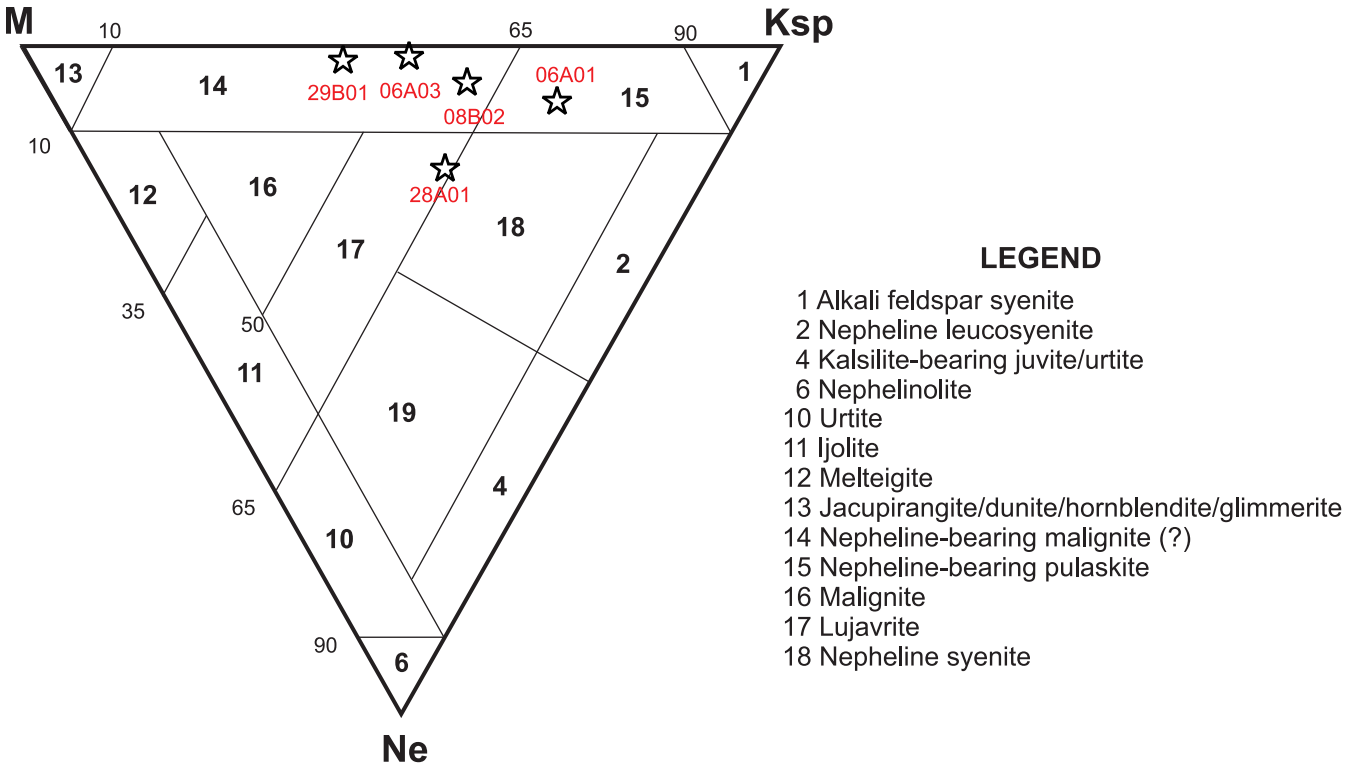

Figure 2. *Preliminary classification of silica-undersaturated rocks, based on modal mineralogy from SEM-MLA analysis (after Lustrino and Bonin, 2024). Sample numbers are abbreviated.*

Table 2. Modal mineralogy of examined samples from SEM-MLA analysis. Red text indicates REE-bearing minerals

Mineral	24RW0006A01 nepheline-bearing pulaskite	24RW0006A03 nepheline-bearing malignite	24RW0008B02 nepheline-bearing malignite	24RW0028A01 lujavrite	24RW0029B01 nepheline-bearing malignite
Albite	36.36	16.67	12.22	38.34	23.16
Orthoclase	30.14	24.98	17.87	6.07	17.86
Nepheline	7.29	0.01	6.17	19.53	1.29
Amphibole	13.90	2.17	21.17	27.89	18.82
Pyroxene	5.53	17.09	28.74	0.21	31.11
Aenigmatite	2.35	0.00	1.35	0.00	0.00
Pectolite	2.30	0.00	0.00	2.01	0.69
Eudialyte	0.30	38.14	9.54	2.97	0.15
Britholite	0.04	0.01	0.01	0.50	2.80
Apatite	0.25	0.00	0.05	0.07	0.00
Synchysite	0.00	0.00	0.00	0.00	0.14
Zr Ca K Si	0.01	0.35	0.08	1.04	1.72
Sodalite	0.47	0.02	0.07	0.10	0.07
Other	1.07	0.55	2.74	1.26	2.19

Table 3. Formulae of the common minerals from the RWIS

Mineral	Formula
Albite	$NaAlSi_3O_8$
Orthoclase	$KAlSi_3O_8$
Nepheline	$Na_3KAl_4Si_4O_{16}$
Arfvedsonite	$(K, Na)_3(Fe^{2+}_4Fe^{3+})Si_8O_{22}(OH,F)_2$
Jadeite	$NaAlSi_2O_6$
Aegirine-Augite	$(Na,Ca)(Fe^{3+},Al^{3+},Mg,Fe^{2+})Si_2O_6$
Aenigmatite	$Na_4Fe^{2+}_{10}Ti_2Si_{12}O_{40}$
Pectolite	$NaCa_2Si_3O_8(OH)$
Eudialyte	$Na_4(Ca,REE)_3(Fe^{2+},Mn)ZrSi_8O_{22}(OH,Cl)$
Britholite	$(REE,Ca)_5(SiO_4,PO_4)_3(OH, F)$
Apatite	$Ca_5(PO_4)_3(Cl,F,OH)$
Synchysite	$CaREE(CO_3)_2F$
Sodalite	$Na_4Si_3Al_3O_{12}Cl$
Fluorite	CaF_2
Galena	PbS
Sphalerite	ZnS
Calcite	$CaCO_3$

ring in the pyroxene-rich malignite (Plate 3A, B). Nepheline occurs in trace amounts. Eudialyte crystallized first followed by K-feldspar, then amphibole and then pyroxene (Plate 3A, C). The K-feldspar is albitized around the rim (Plate 3A). Minor amount of amphibole occurs in the core of pyroxene or around the grain boundaries of eudialyte. Pyroxene surrounds both eudialyte and larger amphibole grains and is zoned with brighter cores and darker rims in BSE images, due to increase in Al and decrease in Fe contents from core to rim (Plate 3D, E). Nepheline formed late and contains inclusions of euhedral pyroxene similar to the rims of the larger pyroxene grains (Plate 3E). Trace amounts of britholite occur as bright needles in nepheline (Plate 3E). An unidentified Zr–Ca–K–silicate occurs around eudialyte.

Sample 24RW0008B02 is a foliated nepheline-bearing malignite containing close to equal amounts of amphibole and pyroxene (Plate 4A, B, Table 2). The main minerals are pyroxene, amphibole, K-feldspar, albite, eudialyte, nepheline and aenigmatite. The order of crystallization is eudialyte and/or aenigmatite, amphibole, pyroxene, K-feldspar, albite and nepheline. Pyroxene is strongly zoned with dark green aegirine–augite core and light green jadeite-rich rim indicating the decrease in Fe and in Al content from core to rim (Plate 4C, D). Nepheline contains euhedral jadeite-rich pyroxene. The main REE mineral is eudialyte, which is altered along cracks (Plate 4E), but trace amounts of britholite are also present.

Sample 24RW0028A01 is an amphibole-rich lujavrite consisting of mainly albite, amphibole, nepheline, K-feldspar, eudialyte, pectolite and an unidentified Ca–K–Zr–Si mineral (Plate 5A, B, Table 2). The sample is foliated and folded (Plate 5A, B) and consists of albite- and nepheline-rich layers, the latter of which contains most of the eudialyte. The order of crystallization is pectolite, eudialyte, albite, amphibole, nepheline and K-feldspar (Plate 5A, C, D). The unidentified Ca–K–Zr–Si mineral occurs around eudialyte, most likely an alteration product after eudialyte. Britholite, occurring in trace amounts, surrounds eudialyte and other minerals suggesting that it crystallized late (Plate 5E). The composition of britholite ranges from Th- and/or Y-bearing and from P-rich and Si-rich. Several unidentified REE-bearing minerals, one of which is also Nb-bearing, occur along veinlets.

Sample 24RW0029B01 is a foliated, pyroxene-rich nepheline-bearing malignite consisting of pyroxene, albite, amphibole, K-feldspar, britholite, nepheline and the unidentified Ca–K–Zr–Si mineral as the main minerals (Plate 6A–C, Table 2). The order of crystallization is pectolite, occurring in minor amounts, followed by K-feldspar, amphibole, pyroxene, albite and nepheline (Plate 6A, C). Most of the K-feldspar occurs as large, eu- to subhedral grains, but also as alteration in albite, indicating K metasomatism (Plate 6A, C, D). Pyroxene displays the usual zoning with a darker Fe-rich core and brighter Al-rich rim in BSE images. Britholite is the main REE mineral in this sample occurring as a late phase and is compositionally variable (Plate 6D, E).

GEOCHEMISTRY

Most samples plot in the nepheline–syenite field, one plots in the ijolite field and a few samples plot in the syenite field (Figure 3A). They are A-type, ferroan and peralkaline, with the agpaitic index ranging up to ~2.9 (average ~1.7) (Figure 3B–D). On the chondrite-normalized spider diagrams, the REE form negative slopes with moderately inclined LREE and weakly inclined or flat HREE patterns, and a strong negative Eu anomaly (Figure 3E).

In the analyzed samples, the Zr content is up to ~1.8 wt. %, the total REE content is up to ~1.4 wt. % (including Y), the total LREE content is up to ~0.8 wt. % and the total HREE content is up to ~0.2 wt. %. The REEs show two positive trends with Zr: a high-Zr, moderate-REE trend well defined by samples containing eudialyte as the main REE mineral and a low-Zr, high-REE trend poorly defined by samples containing britholite as the main REE mineral (Figure 4A). The LREE and HREE are positively correlated displaying two trends parallel to each other: a HREE-poor trend and a HREE-rich trend (Figure 4B) with no apparent correlation to the dominant type of REE mineral in the samples. In addition, the total REE content shows strong positive correlations with As, Mn, Pb and Zn (Figure 4C–F).

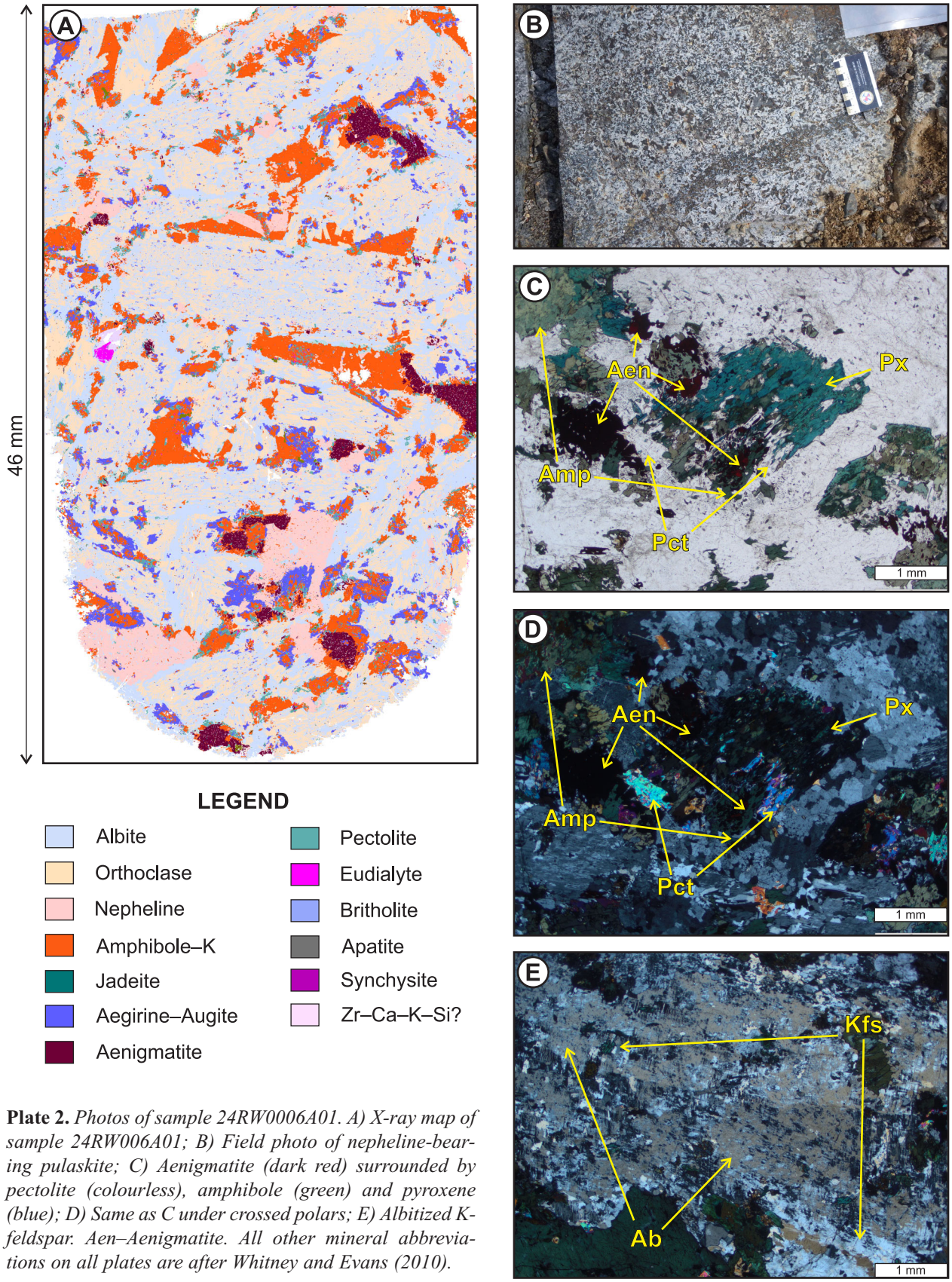

Plate 2. *Photos of sample 24RW0006A01. A) X-ray map of sample 24RW006A01; B) Field photo of nepheline-bearing pulaskite; C) Aenigmatite (dark red) surrounded by pectolite (colourless), amphibole (green) and pyroxene (blue); D) Same as C under crossed polars; E) Albitized K-feldspar. Aen–Aenigmatite. All other mineral abbreviations on all plates are after Whitney and Evans (2010).*

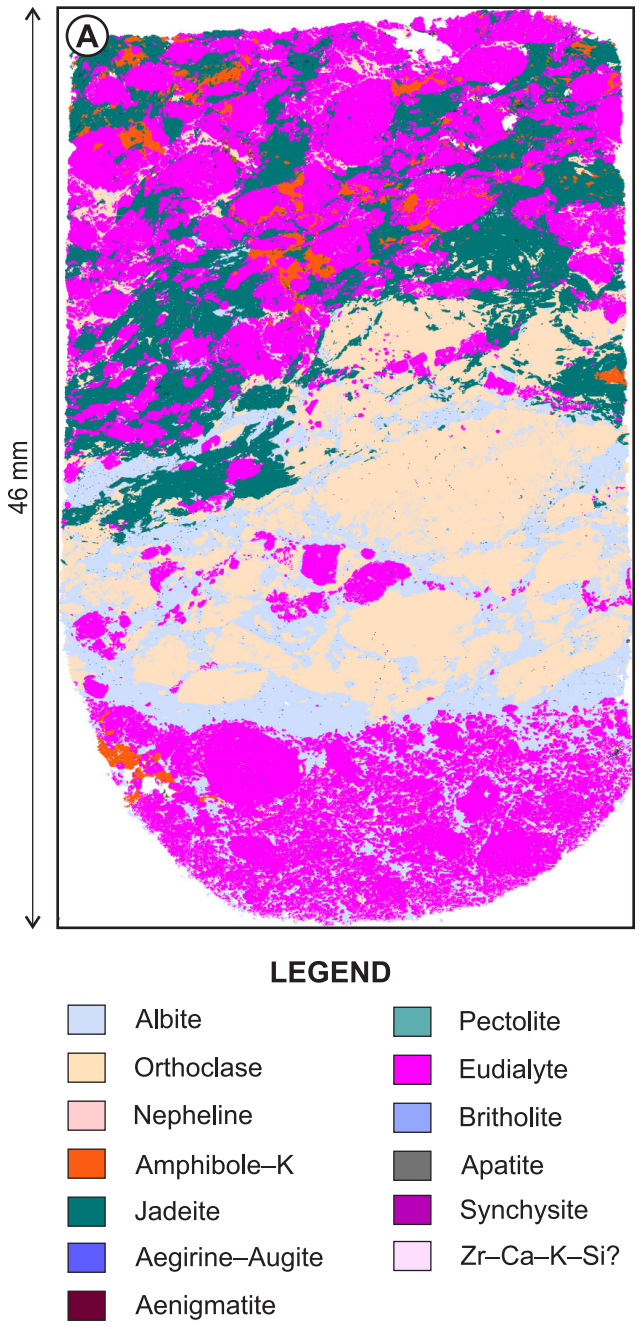

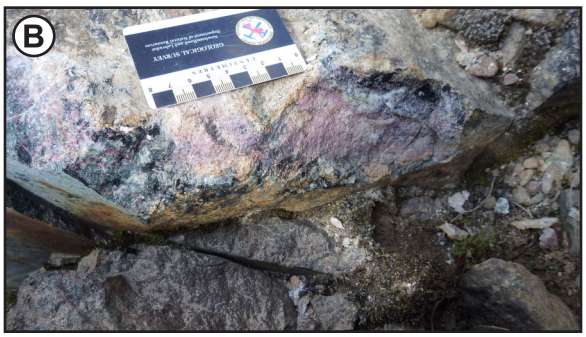

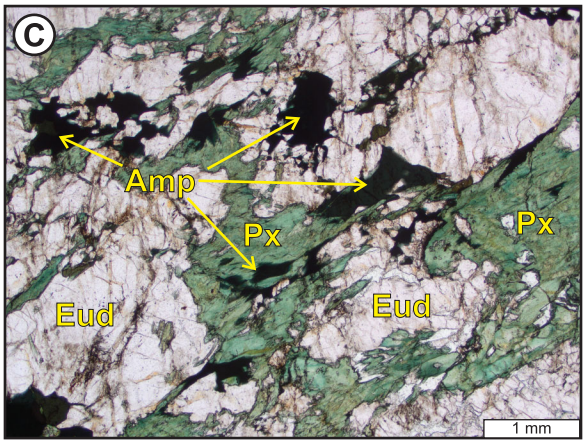

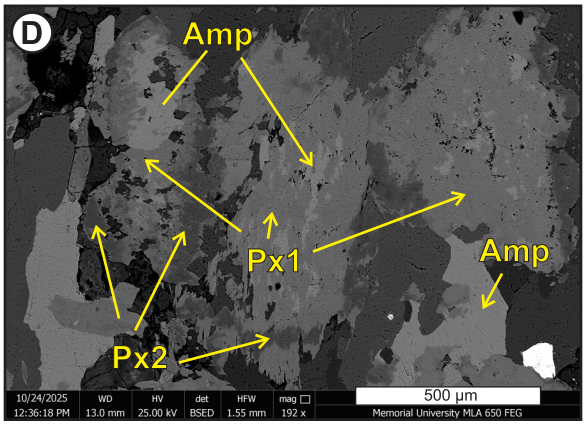

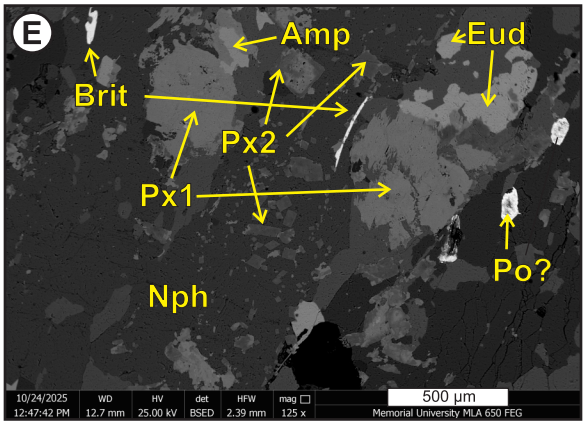

Plate 3. *Photos of sample 24RW0006A03. A) X-ray map of the sample; B) Field photo of eudialyte (pink)-rich layer; C) Eudialyte (light pink) surrounded by amphibole (black) and pyroxene (green); D) BSE image of amphibole surrounded by zoned pyroxene; E) BSE image of zoned pyroxene and nepheline containing inclusions of pyroxene and britholite. Brit–Britholite.*

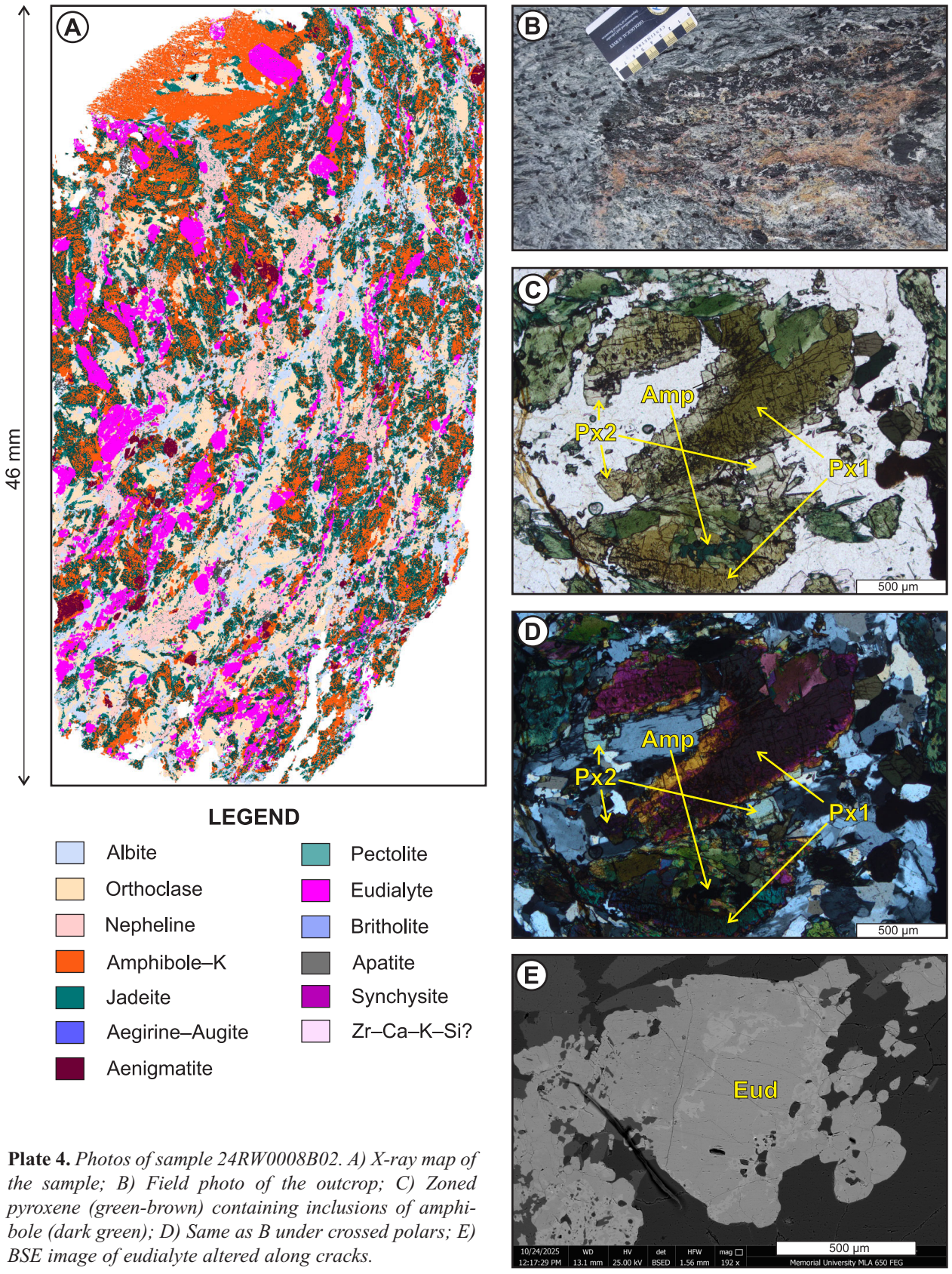

Plate 4. *Photos of sample 24RW0008B02. A) X-ray map of the sample; B) Field photo of the outcrop; C) Zoned pyroxene (green-brown) containing inclusions of amphibole (dark green); D) Same as B under crossed polars; E) BSE image of eudialyte altered along cracks.*

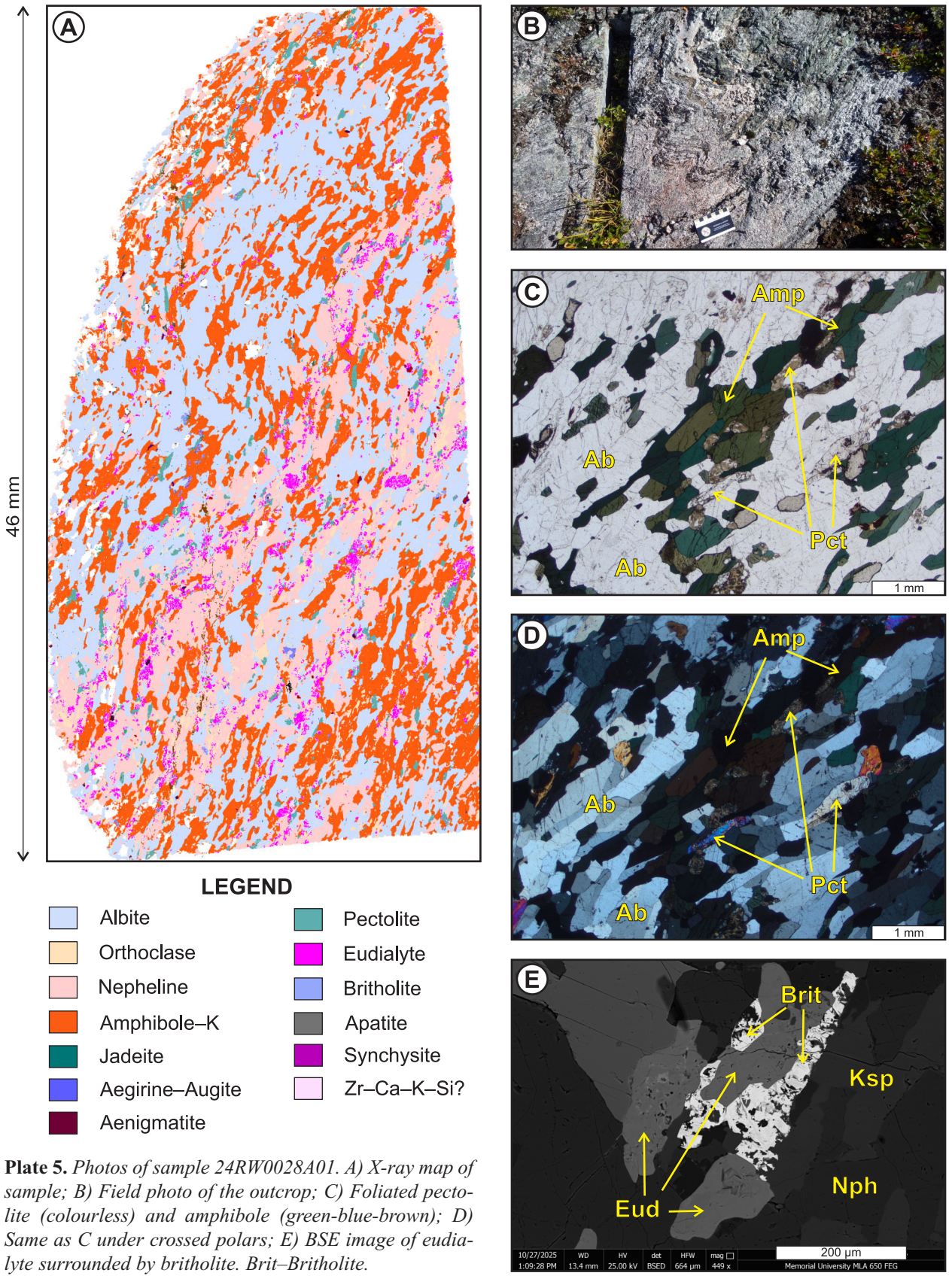

Plate 5. *Photos of sample 24RW0028A01. A) X-ray map of sample; B) Field photo of the outcrop; C) Foliated pectolite (colourless) and amphibole (green-blue-brown); D) Same as C under crossed polars; E) BSE image of eudialyte surrounded by britholite. Brit–Britholite.*

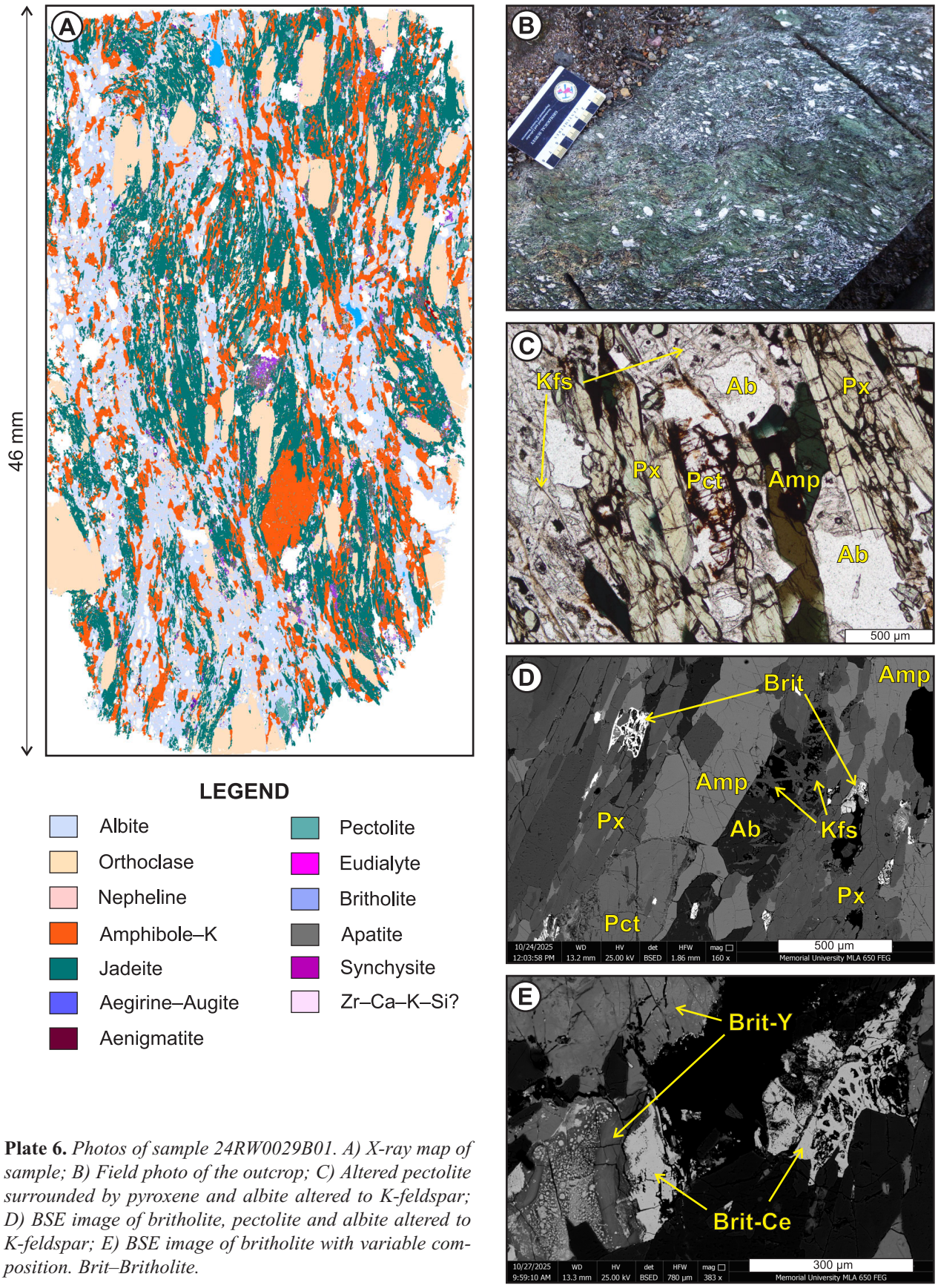

Plate 6. *Photos of sample 24RW0029B01. A) X-ray map of sample; B) Field photo of the outcrop; C) Altered pectolite surrounded by pyroxene and albite altered to K-feldspar; D) BSE image of britholite, pectolite and albite altered to K-feldspar; E) BSE image of britholite with variable composition. Brit–Britholite.*

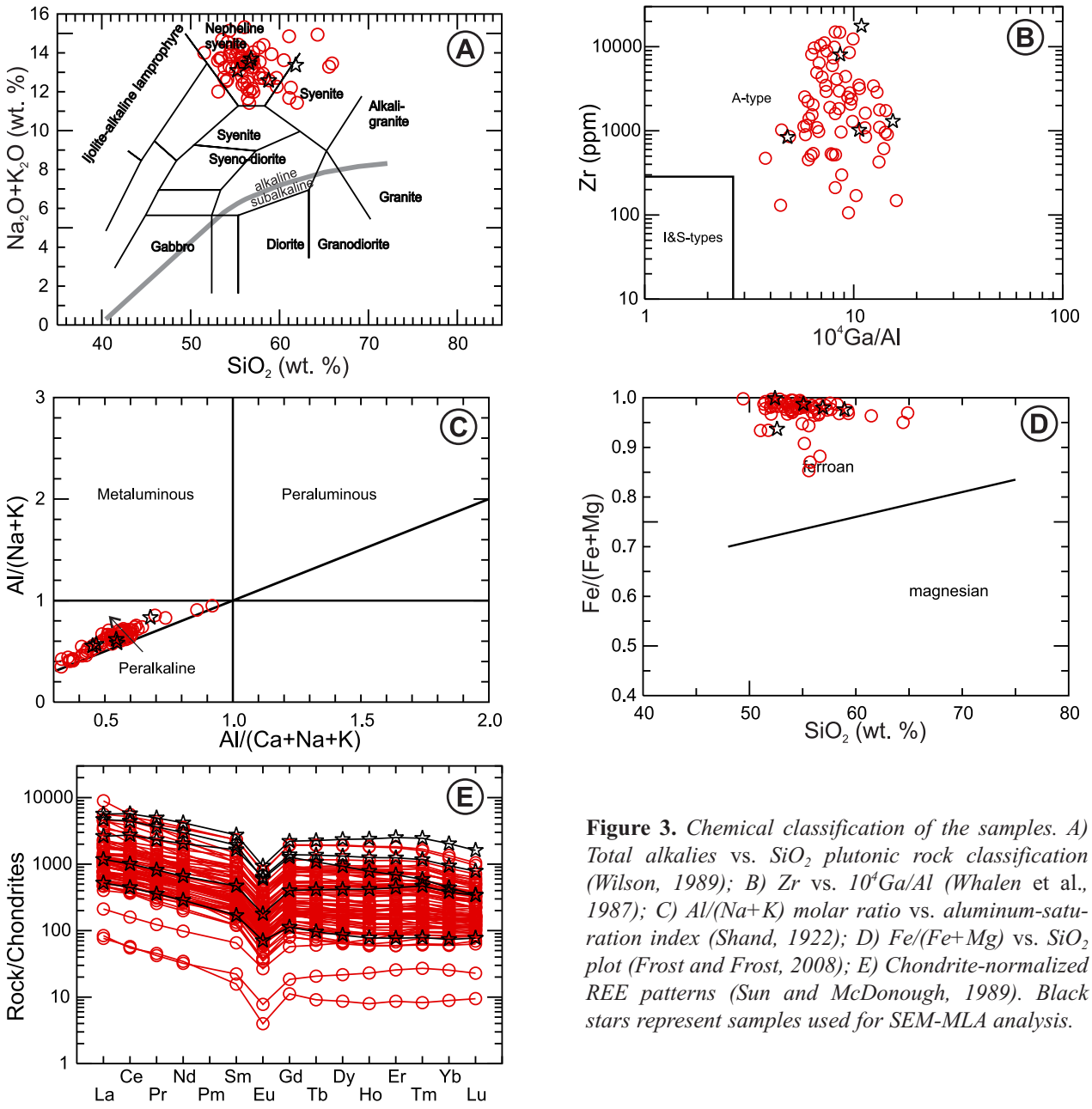

Figure 3. *Chemical classification of the samples. A) Total alkalies* vs. *SiO_2 plutonic rock classification (Wilson, 1989); B) Zr* vs. *10^4Ga/Al (Whalen* et al.*, 1987); C) Al/(Na+K) molar ratio* vs. *aluminum-saturation index (Shand, 1922); D) Fe/(Fe+Mg)* vs. *SiO_2 plot (Frost and Frost, 2008); E) Chondrite-normalized REE patterns (Sun and McDonough, 1989). Black stars represent samples used for SEM-MLA analysis.*

The F content is up to ~4300 ppm and shows a good correlation with FeO (Figure 4G) and MgO in the amphibole-bearing samples, suggesting that most of the F is hosted in amphibole.

DISCUSSION

ROCK TYPES

Based on new SEM-MLA analysis and petrography, the rock types in the NRW pluton of the RWIS are classified as nepheline-bearing pulaskite, nepheline-bearing malignite, lujavrite and malignite. This is partly similar to the rock types described by Curtis and Currie (1981), who reported malignite and lujavrite in the NRW pluton, whereas pulaskite was only described in the SRW. Curtis and Currie (1981) referred to pyroxene-rich lujavrite and malignite as "green melanocratic gneiss" and did not describe amphibole-dominated variants of these rocks. They also described ijolite and melteigite as "blue-black melanocratic gneiss," although these are also more common in the SRW pluton. In this study, only one ijolite was identified in the NRW pluton based on geochemistry (Figure 3A) and melteigite was not found in the NRW pluton.

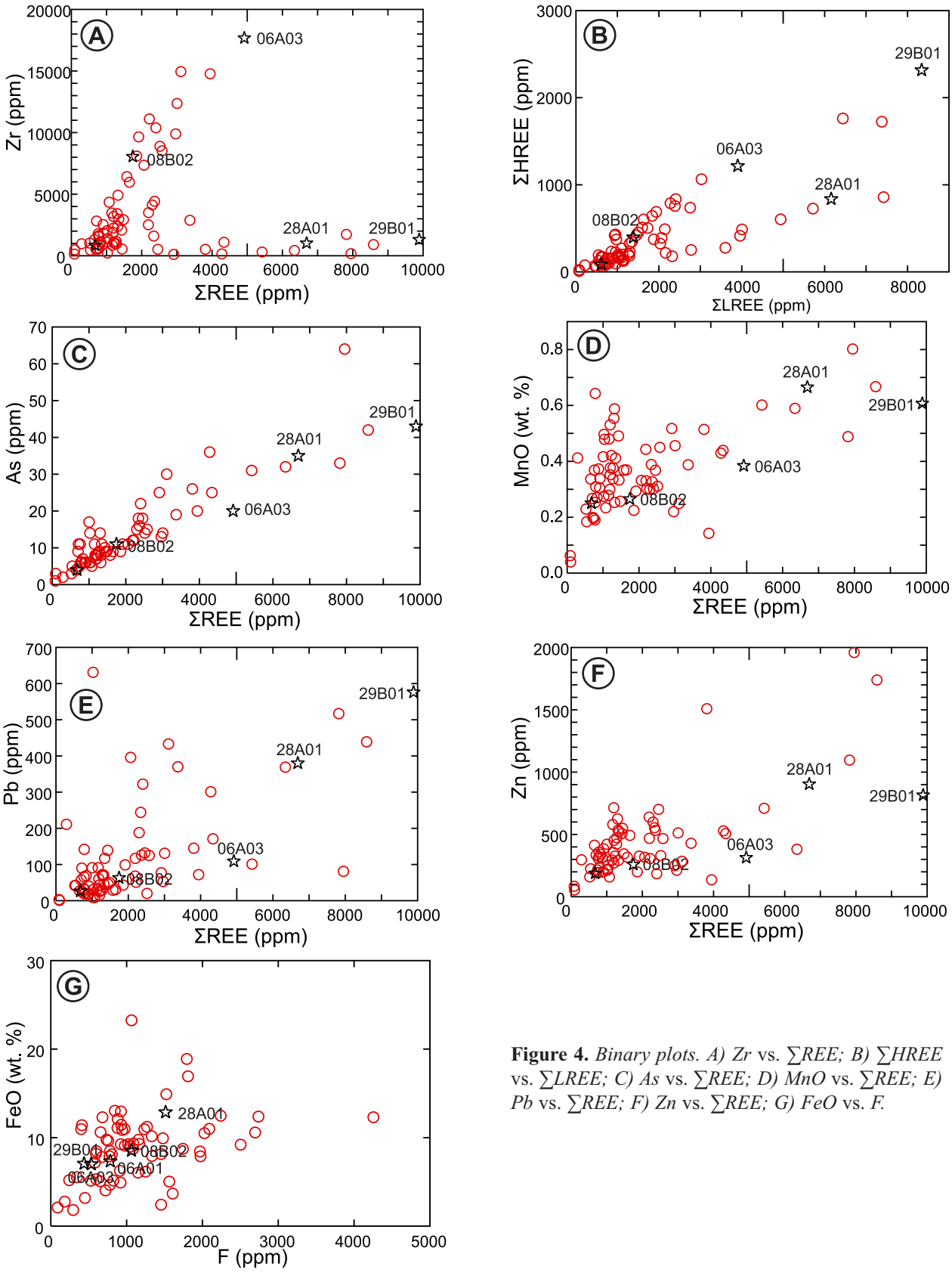

Figure 4. *Binary plots. A) Zr* vs. *∑REE; B) ∑HREE* vs. *∑LREE; C) As* vs. *∑REE; D) MnO* vs. *∑REE; E) Pb* vs. *∑REE; F) Zn* vs. *∑REE; G) FeO* vs. *F.*

The highly variable nature of the pluton is most likely a primary magmatic feature rather than metamorphic. Layering is a typical characteristic of agpaitic intrusions (Bohse and Andersen, 1981; Rose-Hansen and Sørensen, 2002; Bailey *et al.*, 2006; Upton *et al.*, 2013) and may develop due to dynamic processes (mechanical movement of crystals), non-dynamic *in-situ* early magmatic processes (*e.g.*, fractional crystallization) or non-dynamic *in-situ* late or post-magmatic processes (Bailey *et al.*, 2006). Layering can be present at any scale from centimetres to hundreds of metres. Other reasons for the variability of the agpaitic intrusions include intrusions of pegmatites, which may be an early or a late unit, and presence of xenoliths from earlier crystallizing units of the intrusion (Bohse and Andersen, 1981). Alternating aegirine and arfvedsonite layers in the Red Wine rocks are also primary magmatic and reflect changes in physico-chemical (*e.g.*, O fugacity, T, water and silica activity) conditions of the melt (Rose-Hansen and Sørensen, 2002).

DEFORMATION AND METAMORPHISM

The rocks are deformed as clearly indicated by widespread foliation, lineation and folding. However, some of the fabric may also reflect primary features. Lamination of feldspars is due to feldspar being a cumulus phase in syenites, and even lineations of amphibole are typical in undeformed agpaitic intrusions as observed in Greenland (Upton *et al.*, 1996, 2013; Rose-Hansen and Sørensen, 2002).

The grade of metamorphism in the RWIS was estimated at amphibolite facies based on the increase in Al and decrease in Fe content of the pyroxene from core to rim, and the co-existence of jadeitic pyroxene with nepheline and albite (Curtis and Currie, 1981). This is in contrast with the metamorphic grade in the surrounding rocks. The grade of metamorphism ranges up to upper greenschist in both the LLG, which is around the same age as the RWIS, and the older Trans-Labrador batholith (Thomas, 1981). To account for this inconsistency, Curtis and Currie (1981) suggested that rocks of the RWIS were transported upward from deeper levels along thrust faults. They also note that the grade of metamorphism changes drastically over very short distances (few cm), which they explain with mechanical reworking, although no evidence is presented to support this explanation.

Several studies linked the presence of Al-rich jadeitic rims of pyroxenes to metamorphism (*e.g.*, Norra Kärr in Atanasova *et al.*, 2017), but Chakrabarty *et al.* (2016) argues that jadeitic pyroxene in the agpaitic Sushina Hill Complex is most likely related to subsolidus processes that took place at temperatures similar to greenschist- to lower-amphibolite-facies metamorphism. Although jadeite is a characteristic mineral in blue-schist facies rocks, it can also form in silica-deficient environments at ≤5 kbar pressures and temperatures between 350 and 700°C (Chakrabarty *et al.*, 2016 and references within). Also, jadeite-rich pyroxene has been reported from the unmetamorphosed Ilímaussaq complex (Markl *et al.*, 2001). Chakrabarty *et al.* (2016) concluded that subsolidus processes in agpaitic rocks in the Sushina Hill Complex are near-impossible to distinguish from metamorphic processes at greenschist to lower-amphibolite facies.

The coexistence of nepheline and jadeite as another evidence for amphibolite-grade metamorphism (Curtis and Currie, 1981) is also questionable. In the present study, nepheline, in some of the samples, contains inclusions of amphibole in addition to jadeitic pyroxene (Plate 2A), which is interpreted here as primary magmatic nepheline crystallizing after both of these phases. Therefore, it is possible that the RWIS underwent only greenschist-facies metamorphism, similar to the metamorphic grade attained by the surrounding geological units and was not transposed from deeper crustal levels as suggested by Curtis and Curry (1981).

REE MINERALIZATION

Two distinct types of mineralization occur in the NRW: one dominated by eudialyte and the other by britholite (Crocker, 2014). The eudialyte-rich mineralization is interpreted as primary magmatic, indicated by the early crystallization of eudialyte. In contrast, the britholite-rich mineralization is later and most likely hydrothermal, as suggested by textural relationships, and the weak correlation between REE and Zr (Figure 4A). Both Zr and REE are incompatible elements that typically increase with fractional crystallization. Therefore, the weak correlation implies another process of REE enrichment, most likely late magmatic hydrothermal, which is common in agpaitic rocks due to their very high volatile content. The samples examined in this study show evidence of both sodium (Plates 2E and 3A) and potassium metasomatism (Plate 6C, D).

CONCLUSIONS

The RWIS represents the most evolved Mesoproterozoic, REE-mineralized alkaline-silicate system in Labrador, indicating its significant potential for hosting economically important mineralization. Despite numerous studies since its discovery in the 1950s, the suite remains poorly understood due to the rarity of these rocks and the added complexity introduced by subsequent metamorphism and deformation.

This report presents a detailed investigation of representative rock types from the NRW, including SEM-MLA data not previously applied here. This is an important step, because historically, rock identification and nomenclature

has been challenging due to the uncommon nature of the rocks and also limited understanding of metamorphic overprints, often resulting in mixed igneous and metamorphic terminology (Curtis and Currie, 1981). Comparisons with other agpaitic intrusions suggest that some features previously attributed to deformation may be primary magmatic structures, and the metamorphic grade may have been overestimated.

Future work will include Nd–Sm isotopic studies to constrain the source of the rocks and early processes such as crustal contamination, mineral chemistry and whole-rock chemistry to unravel the various processes (igneous, hydrothermal and metamorphic) and relative timing of the units, and further geochronology concentrating of the RWO and LLG, which are less difficult to date than the RWU.

ACKNOWLEDGMENTS

The authors are grateful for the assistance of Dylan Goudie with the SEM/SEM-MLA analysis at MUN. Joanne Rooney and Evie Li from GSNL are thanked for typesetting and cartography support, respectively. The paper was improved by the careful review of James Conliffe, GSNL.

REFERENCES

Atanasova, P., Marks, M.A.W., Heinig, T., Krause, J. Gutzmer, J. and G. Markl, G.
2017: Distinguishing magmatic and metamorphic processes in peralkaline rocks of the Norra Kärr Complex (Southern Sweden) using textural and compositional variations of clinopyroxene and eudialyte-group minerals. Journal of Petrology, Volume 58, pages 361-384. https://doi.org/10.1093/petrology/egx019

Bailey, J.C., Sørensen, H., Andersen, T., Kogarko, L.N. and Rose-Hansen, J.
2006: On the origin of microrhythmic layering in arfvedsonite lujavrite from the Ilímaussaq alkaline complex, South Greenland. Lithos, Volume 91, pages 301-318. https://doi.org/10.1016/j.lithos.2006.03.022

Beard, C.D., Goodenough, K.M., Borst, A.M., Wall, F., Siegfried, P.R., Deady, E.A., Pohl, C., Hutchison, W., Finch, A.A., Walter, B.F., Elliott, H.A.L. and Brauch, K.
2022: Alkaline-silicate REE-HFSE systems. Economic Geology, Volume 118, pages 177-208. https://doi.org/10.5382/econgeo.4956

Blaxland, A.B. and Curtis, L.C.
1977: Chronology of the Red Wine alkaline province, central Labrador. Canadian Journal of Earth Sciences, Volume 14, pages 1940-1946.

Bohse, H. and Andersen, S.
1981: Review of the stratigraphic divisions of the kakortokite and lujavrite in southern Ilímaussaq. Rapport-Grønlands Geologiske Undersøgelse, Volume 103, pages 53-62.

Cadman, A.C., Heaman, L.M., Tarney, J., Wardle, R.J. and Krogh, T.E.
1993: U–Pb geochronology and geochemical variation within two Proterozoic mafic dyke swarms, Labrador. Canadian Journal of Earth Sciences, Volume 30, pages 1490-1504.

Chakrabarty, A., Mitchell, R., Ren, M., Saha, P., Pal, S., Pruseth, K. and Sen, A.
2016: Magmatic, hydrothermal and subsolidus evolution of the agpaitic nepheline syenites of the Sushina Hill Complex, India: Implications for the metamorphism of peralkaline syenites. Mineralogical Magazine, Volume 80, pages 1161-1193.

Crocker, M.G.
2014: A petrographic, geochemical and geochronological study of rare earth mineralization in the Red Wine Intrusive Suite, Labrador, Canada. Unpublished M.Sc. thesis, Memorial University of Newfoundland, St. John's, Newfoundland, 766 pages.

Curtis, L. and Currie, K.L.
1981: Geology and petrology of the Red Wine alkaline complex, central Labrador. Geological Survey of Canada, Bulletin 294, 61 pages.

Curtis, L. and Gittins, J.
1979: Aluminous and titaniferous clinopyroxenes from regionally metamorphosed agpaitic rocks in central Labrador. Journal of Petrology, Volume 20, pages 165-186.

Daigle, P.
2012: Resource estimate and technical report for the Two Tom REE deposit of the Red Wine Complex, Labrador, Canada. Rare Earth Metals Inc., 163 pages.

Ducharme, T.A., McFarlane, C.R.M., van Rooyen, D. and Corrigan, D.
2021: Petrogenesis of the peralkaline Flowers River Igneous Suite and its significance to the development of the southern Nain Batholith. Geological Magazine, Volume 168, pages 1911-1936.

Finch, C., Roldan, R., Walsh, L., Kelly, J. and Amor, S.
2018: Analytical methods for chemical analysis of geological materials. Government of Newfoundland and

Labrador, Department of Natural Resources, Geological Survey, Open File NFLD/3316, 67 pages.

Frost, B.R. and Frost, C.D.
2008: A geochemical classification for feldspathic igneous rocks. Journal of Petrology, Volume 49, pages 1955-1969. https://doi.org/10.1093/petrology/egn054

Fryer, B.J.
1983: Report on geochronology, Labrador mapping. Government of Newfoundland and Labrador, Department of Mines and Energy, Mineral Development Division, Open File LAB 617, 35 pages.

Gandhi, S.S., Krogh, T.E. and Corfu, F.
1988: U-Pb zircon and titanite dates on two granitic intrusions of the Makkovik Orogen and a peralkaline granite of the Red Wine Intrusive Complex, central Labrador. Geological Association of Canada–Mineralogical Association of Canada–Canadian Society of Petroleum Geologists, Program with Abstracts, Volume 13, page A42.

Gower, C.F., Ryan, A.B., Bailey, D.G. and Thomas, A.
1980: The position of the Grenville front in eastern and central Labrador. Canadian Journal of Earth Sciences, Volume 17, pages 784-788.

Hill, J.D. and Miller, R.R.
1990: A review of middle Proterozoic epigenic felsic magmatism in Labrador. *In* Mid-Proterozoic Laurentia-Baltica. *Edited by* C.F. Gower, T. Rivers and B. Ryan. Geological Association of Canada, Special Paper 38, pages 417-431.

Hill, J.D. and Thomas, A.
1983: Correlation of two Helikian peralkaline granite-volcanic centres in central Labrador. Canadian Journal of Earth Sciences, Volume 20, pages 753-763.

Le Maitre, R.W., Streckeisen, A., Zanettin, B., Le Bas, M.J., Bonin, B. and Bateman, P. (eds.)
2002: Igneous Rocks: A Classification and Glossary of Terms: Recommendations of the International Union of Geological Sciences Subcommission on the Systematics of Igneous Rocks. 2nd ed. Cambridge University Press.

Lustrino, M. and Bonin, B.
2024: A revision of the IUGS recommendations for classification and nomenclature of igneous rocks - A preliminary report.
https://doi.org/10.13140/RG.2.2.16849.54883

Magyarosi, Z. and Rayner, N.
2025: New geochronology data from the REE occurrences and associated rocks in the Port Hope Simpson–St. Lewis area, southeastern Labrador. *In* Current Research. Government of Newfoundland and Labrador, Department of Industry, Energy and Technology, Geological Survey, Report 25-1, pages 45-62.

Markl, G., Marks, M.A., Schwinn, G. and Sommer, H.
2001: Phase equilibrium constraints on intensive crystallization parameters of the Ilímaussaq Complex, South Greenland. Journal of Petrology, Volume 42, pages 2231-2257.
https://doi.org/10.1093/petrology/42.12.2231

Marks, M.A.W. and Markl, G.
2017: A global review on agpaitic rocks. Earth-Science Reviews, Volume 173, pages 229-258.
https://doi.org/10.1016/j.earscirev.2017.06.002

Mikhailova, J.A., Pakhomovsky, Y.A., Panikorovskii, T.L., Bazai, A.V. and Yakonvenchuk, V.N.
2020: Eudialyte group minerals from the Lovozero Alkaline Massif, Russia: Occurrence, chemical composition, and petrogenetic significance. Minerals, Volume 10. http://dx.doi.org/10.3390/min10121070

Miller, R.R.
1987: Relationship between Mann-type Nb–Be mineralization and felsic peralkaline intrusives, Letitia Lake project, Labrador. *In* Current Research. Government of Newfoundland and Labrador, Department of Mines and Energy, Mineral Development Division, Volume 87-1, pages 83-91.

Miller, R.R., Heaman, L.M. and Birkett, T.C.
1997: U–Pb zircon age of the Strange Lake peralkaline complex: Implications for Mesoproterozoic peralkaline magmatism in north-central Labrador. Precambrian Research, Volume 81, pages 67-82.

Romer, R.L., Schärer, U., Wardle, R.J. and Wilton, D.H.C.
1995: U–Pb age of the Seal Lake Group, Labrador: Relationship to Mesoproterozoic extension-related magmatism of Laurasia. Canadian Journal of Earth Sciences, Volume 32, pages 1401-1410.

Rose-Hansen, J. and Sørensen, H.
2002: Geology of the lujavrites from the Ilímaussaq alkaline complex South Greenland, with information from seven bore holes. Contribution to the Mineralogy of Ilímaussaq no. 109, Meddelelser om Grønland Geoscience, Volume 40, Copenhagen, Danish Polar Center, 2002.

Shand, S.J.
1922: The problem of the alkaline rocks. Proceedings of the Geological Society of South Africa, Volume 25, pages 19-33.

Singh, K.S.
1972: Petrological and mineralogical studies of the Joan Lake agpaitic complex, central Labrador. Ph.D. thesis.. University of Ottawa, Ottawa, Ontario, 207 pages.

Sun, S.S. and McDonough, W.F.
1989: Chemical and isotopic systematics of oceanic basalts: implications for mantle composition and processes. *In* Magmatism in the Ocean Basins. *Edited by* A.D. Saunders and M.J. Norry. Geological Society of London, Special Publication 42, pages 313-345.

Thomas, A.
1981: Geology along the southwestern margin of the Central Mineral Belt. Government of Newfoundland and Labrador, Department of Mines and Energy, Mineral Development Division, Report 81-4, 40 pages.

1993: Geology of the Red Wine Mountains and surrounding area, north central Grenville Province, Labrador. Government of Newfoundland and Labrador, Department of Mines and Energy, Geological Survey Branch, Open File LAB/0989, 321 pages.

Upton, B.G.J., Macdonald, R., Odling, N., Rämö, O.T. and Bagiński, B.
2013: Kûngnât, revisited: A review of five decades of research into an alkaline complex in South Greenland, with new trace-element and Nd isotopic data. Mineralogical Magazine, Volume 77, pages 523-550. https://doi.org/10.1180/minmag.2013.077.4.11

Upton, B.G.J., Parsons, P., Emeleus, C.H. and Hodson, M.E.
1996: Layered alkaline igneous rocks of the Gardar Province, South Greenland. Developments in Petrology, Volume 15, pages 331-363.

van Nostrand, T. and Corcoran, C.
2013: Geology of the western Mesoproterozoic Seal Lake Group, central Labrador (including all of NTS map areas 13L/2 and 7 and parts of 13L/1, 3, 6, 8, 9, 10, 11, 14, 15 and 16 and 13E/14 and 15). *In* Current Research. Government of Newfoundland and Labrador, Department of Natural Resources, Geological Survey, Volume 13-1, pages 301-326.

Vasyukova, O.E. and Williams-Jones, A.E.
2018: Direct measurement of metal concentrations in fluid inclusions, a tale of hydrothermal alteration and REE ore formation from Strange Lake, Canada. Chemical Geology, Volume 483, pages 385-396. https://doi.org/10.1016/j.chemgeo.2018.03.003

Wardle, R.J., Gower, C.F., Ryan, B., Nunn, G.A.G., James, D.T. and Kerr, A.
1997: Geological map of Labrador; 1:1 million scale. Government of Newfoundland and Labrador, Department of Mines and Energy, Geological Survey, Map 97-07.

Whalen, J.B., Currie, K.L. and Chappell, B.W.
1987: A-type granites: geochemical characteristics, discrimination and petrogenesis. Contributions to Mineralogy and Petrology, Volume 95, pages 407-419.

Whitney, D.L. and Evans, B.W.
2010: Abbreviations for names of rock-forming minerals. American Mineralogist, Volume 95, pages 185-187.

Wilson, M.
1989: Igneous Petrogenesis: A Global Tectonic Approach. Unwin Hyman, London, 466 pages. https://doi.org/10.1007/978-1-4020-6788-4